

TIGHTLY FOCUSED LASER LIGHT WITH AZIMUTHAL POLARIZATION AND SINGULAR PHASE

V.V. Kotlyar^{1,2}, A.G. Nalimov^{1,2}

¹Image Processing Systems Institute of RAS, – Branch of the FSRC “Crystallography and Photonics” RAS, Samara, Russia,

²Samara National Research University, Samara, Russia

Abstract

Using simplified Richards-Wolf formulas we show that laser light with azimuthal polarization and singular phase can produce a smaller focal spot than that from a laser beam with radial polarization, other conditions remaining the same. It is numerically shown that when focusing an azimuthally polarized laser beam with phase singularity using a zone plate a 1.3 times smaller focal spot can be attained than when an aplanatic lens is used. A spiral phase plate can be replaced with a phase step with a π -phase shift. In this case the subwavelength focal spot from a laser beam with azimuthal polarization, which is formed near the zone plate surface, loses circular symmetry, while becoming smaller and acquiring an elliptical form with radiuses of 0.273λ and 0.314λ ($NA = 1$).

Keywords: zone plate, polarization conversion, diffraction grating.

Citation: Kotlyar VV, Nalimov AG. Tightly focused laser light with azimuthal polarization and singular phase. *Computer Optics* 2016; 40(5): 642-648. DOI: 10.18287/2412-6179-2016-40-5-642-648.

Acknowledgements: This work was partially funded by the Russian Foundation for Basic Research (RFBR) grants ## 14-29-07133, 15-07-01174, 16-29-11698, 16-47-630483; Russian Federation Ministry of Education and Science; Russian Federation Presidential grants for support of leading scientific schools (NSH-9498.2016.9).

Introduction

It has been numerically shown [1] that a Bessel-Gauss laser beam with azimuthal polarization having passed through a spiral phase plate (SPP) with the unit topological charge forms at the focus of a high-NA lens a subwavelength circular focal spot that is smaller in diameter than for radially polarized incident light. Using the Richards-Wolf formulas [2], it was also shown [1] that for an aplanatic spherical lens with $NA=1.4$ (immersion with a refractive index of $n=1.518$), for the azimuthal polarization and singular phase the focal spot size at half intensity was $FWHM=0.34\lambda$, whereas radially polarized light produced the focal spot of size $FWHM=0.40\lambda$ in the same conditions, λ is the wavelength in vacuum [3]. However, no final formulas to describe the intensity of azimuthally polarized light, transmitted through an SPP, in the focus of the aplanatic lens were proposed in [1-3]. In [4], it was numerically and experimentally found that a Bessel-Gauss laser beam with azimuthal polarization having passed through a SPP and a focused by a lens with $NA=1.4$ produced a focal spot of size $FWHM=0.25\lambda$. This is certainly a fairly good result, but it does not correspond with the results reported in [1, 3].

In [4] an incomplete formula for the electric field vector in the focus of the lens for an azimuthally polarized laser beam having passed through a SPP was proposed. In that formula, there was an explicit azimuthal dependence of the amplitude and the focal spot was shown not to be circular. Other known papers reported studies of the tight focus of inhomogeneously polarized laser vortex beams (with radial and azimuthal polarization) by means of phase diffractive optical elements with a singular phase [5,6]. The size of the focal spot can be further reduced using a circular aperture [7,8].

In this paper, we show that the intensity distribution in the focus of an aplanatic lens from an azimuthally po-

larized laser beam having passed through a SPP is radially symmetric. Based on the derived relations, we qualitatively show that the diameter of the focal spot from an azimuthally polarized field with singular phase is smaller than that from a radially polarized field, other conditions remaining the same. Also, we show numerically that by replacing the SPP with a phase step with the π -phase delay an elliptical focal spot of a smaller size is found in the focus of the zone plate, instead of a circular one. Note that the sharp focus of a laser beam with linear polarization having passed through a phase step with π -phase delay was considered in [9].

Theoretical comparison of focusing light beams with radial and azimuthal polarizations

The electric field vector of a coherent electromagnetic wave in the focus of an aplanatic lens is given by [2,3]:

$$\mathbf{E}(r, \varphi, z) = i \int_0^{\theta_0} \int_0^{2\pi} \sin \theta E(\theta) \cos^{1/2} \theta \mathbf{T}(\theta, \psi) \mathbf{P}(\psi) \times \exp \left[ikn(z \cos \theta + r \sin \theta \cos(\varphi - \psi)) \right] d\theta d\psi, \quad (1)$$

where (r, φ, z) are cylindrical coordinates in the focal plane, (θ, ψ) are the polar and azimuthal angles between the geometrical focus point and the exit pupil of the aplanatic lens, k is the wave number, n is the refractive index of the medium in the focal plane, and $\theta_0 = \arcsin\left(\frac{NA}{n}\right)$ is the angle aperture of the lens. The complex amplitude of an incident wave, for example, a Bessel-Gauss beam can be found as:

$$E(\theta) = E_0 \exp \left[-\left(\frac{\beta \sin \theta}{\sin \theta_0} \right)^2 \right] \times J_1 \left(\frac{2\beta \sin \theta}{\sin \theta_0} \right), \quad (2)$$

where β – parameter equal to the ratio of the radius of the pupil of the lens to the radius of the laser beam waist.

Matrix 3x3 in (1) can be expressed as:

$$\mathbf{T}(\theta, \psi) = \begin{bmatrix} \sin^2 \psi + \cos \theta \cos^2 \psi & \cos \psi \sin \psi (\cos \theta - 1) & -\sin \theta \cos \psi \\ \cos \psi \sin \psi (\cos \theta - 1) & \cos^2 \psi + \cos \theta \sin^2 \psi & -\sin \theta \sin \psi \\ \sin \theta \cos \psi & \sin \theta \sin \psi & \cos \theta \end{bmatrix}. \tag{3}$$

The polarization vector of the incident light field in (1) can be found as:

$$\mathbf{P}(\psi) = [-\sin \psi, \cos \psi, 0] \tag{4}$$

for azimuthal polarization and

$$\mathbf{P}(\psi) = [\cos \psi, \sin \psi, 0] \tag{5}$$

for radial polarization.

Substituting (4) in (1) and taking into account (3), we find that for the azimuthal polarization only one azimuthal projection of the electric vector contributes to the focal spot (with the other projections being equal to zero):

$$E_\phi(r, z) = 2\pi i \int_0^{\theta_0} \sin \theta \cos^{1/2} \theta E(\theta) \times \tag{6}$$

$$\times J_1(krn \sin \theta) \exp(iknz \cos \theta) d\theta,$$

where $J_1(x)$ is the Bessel function of the first order.

It can be seen from (6) that a bright ring with an intensity null on the optical axis is formed.

To obtain an intensity maximum on the axis it was proposed in [1] that the lens be illuminated by azimuthally polarized light having passed through a SPP with transmittance $F(\psi) = \exp(im\psi)$, where $m=1$. In this case instead of the function $E(\theta)$ in (1) the function $E(\theta) = \exp(i\phi)$ needs to be considered. Then from (6) we obtain only two transverse Cartesian coordinates of the electric vector:

$$E_x(r, \phi, z) = \pi \int_0^{\theta_0} \sin \theta \cos^{1/2} \theta E(\theta) \times \tag{7}$$

$$\times [e^{2i\phi} J_2(krn \sin \theta) + J_0(krn \sin \theta)] \times$$

$$\times \exp(iknz \cos \theta) d\theta,$$

$$E_y(r, \phi, z) = \pi i \int_0^{\theta_0} \sin \theta \cos^{1/2} \theta E(\theta) \times \tag{8}$$

$$\times [e^{2i\phi} J_2(krn \sin \theta) - J_0(krn \sin \theta)] \times$$

$$\times \exp(iknz \cos \theta) d\theta.$$

Expression similar to (7) and (8), but incomplete, were derived in [4]. It is seen from (7) and (8) that the complex amplitude explicitly depends on the azimuthal angle ϕ . That is, it is not clear from these formulas, whether or not the focal spot is circular. However, if we write the expression for the intensity in the focal plane (at $z=0$), the circular symmetry of the focal spot is obvious:

$$I_{az}(r) = |E_x|^2 + |E_y|^2 = \tag{9}$$

$$= 2 \left| \pi \int_0^{\theta_0} \sin \theta \cos^{1/2} \theta E(\theta) J_2(krn \sin \theta) d\theta \right|^2 +$$

$$2 \left| \pi \int_0^{\theta_0} \sin \theta \cos^{1/2} \theta E(\theta) J_0(krn \sin \theta) d\theta \right|^2.$$

For comparison, we write down the non-zero projection of the electric vector for the radially polarized light field in focus, derived from (1), (3) and (5):

$$E_r(r, \phi, z) = -2\pi \int_0^{\theta_0} \sin \theta \cos^{3/2} \theta E(\theta) \times \tag{10}$$

$$\times J_1(krn \sin \theta) \exp(iknz \cos \theta) d\theta,$$

$$E_z(r, \phi, z) = 2\pi i \int_0^{\theta_0} \sin^2 \theta \cos^{1/2} \theta E(\theta) \times \tag{11}$$

$$\times J_0(krn \sin \theta) \exp(iknz \cos \theta) d\theta.$$

From (10) and (11), the radially polarized field is seen to have in the focus only two projections of the electric vector: the transverse radial and longitudinal axial ones. From (10) and (11) we obtain the intensity distribution in the focal plane ($z=0$) for the radial field:

$$I_{rad}(r) = |E_r|^2 + |E_z|^2 = \tag{12}$$

$$= 4 \left| \pi \int_0^{\theta_0} \sin \theta \cos^{3/2} \theta E(\theta) J_1(krn \sin \theta) d\theta \right|^2 +$$

$$4 \left| \pi \int_0^{\theta_0} \sin^2 \theta \cos^{1/2} \theta E(\theta) J_0(krn \sin \theta) d\theta \right|^2.$$

From the comparison of (9) and (12) it is difficult to determine which of the foci is smaller in diameter (for a radially polarized beam or an azimuthally polarized beam with singular phase). Although in front of the terms in (12) is four, and (9) - two, the terms themselves are different. In the second term in (9) and (12) is the same zero-order Bessel function, but in (12) there is the sine squared, which gives a smaller area under the curve than when a sine function is used. Therefore, a two-times difference in the coefficients can be compensated due to different integrands. The same applies to the first term in (9) and (12).

In (9) is the second-order Bessel function, in which the area under the curve is smaller than that of the first-order Bessel function, which is the first term in (12), but the cosine in (12) to the power 3/2 has a smaller area, than cosine to the power 1/2, which is found in (9). It is possible to accurately calculate the maximum intensity at the focus of the two beams (9) and (12) when the lens is illuminated by a plane wave with a unit amplitude and maximum numerical aperture in free space: $E(\theta)=1$ and $\theta_0=\pi/2$.

Then, (9) and (12) on the optical axis (at $r=0$) take the form:

$$I_{az}(r=0) = 2 \left| \pi \int_0^1 \xi (1-\xi^2)^{-1/4} d\xi \right|^2 = 2\pi^2 \left(\frac{2}{3} \right)^2, \tag{13}$$

$$I_{rad}(r=0) = 4 \left| \pi \int_0^1 \xi^2 (1-\xi^2)^{-1/4} d\xi \right|^2 = \tag{14}$$

$$= 4\pi^2 \left[\frac{\Gamma(3/2)\Gamma(3/4)}{2\Gamma(9/4)} \right]^2.$$

From (13) and (14) it follows that the ratio of these intensities is nearly equal to 1:

$$I_{az}/I_{rad} = 0.9673. \tag{15}$$

It can be concluded that the second terms in (9) and (12) give almost the same and the main contributions to the focus size, and if there is a difference in the size of both foci, it is determined by the first terms in (9) and (12).

It can be evaluated qualitatively which of the first terms in (9) and (12) drops faster with increasing radial coordinate. For this we use a reference integral [10]:

$$\int_0^a x^{\alpha-1} (a^2 - x^2)^{\beta-1} J_\nu(cx) dx = \frac{a^{2\beta+\alpha+\nu-2} c^\nu}{2^{\nu+1}} \frac{\Gamma(\beta)\Gamma((\alpha+\nu)/2)}{\Gamma((\alpha+\nu)/2+\beta)\Gamma(\nu+1)} \times {}_1F_2((\alpha+\nu)/2, (\alpha+\nu)/2+\beta, \nu+1, -a^2c^2/4). \tag{16}$$

In (16), $\Gamma(x)$ is the gamma function and the hypergeometric function is given by [11]

$${}_1F_2(b, c, d, x) = \sum_{k=0}^{\infty} \frac{(b)_k x^k}{(c)_k (d)_k k!}, \tag{17}$$

$$(b)_k = b(b+1)\dots(b+k-1).$$

The first term in (9) is proportional to the square of the integral ($E(\theta) = 1$ and $\theta_0 = \pi/2$):

$$\int_0^1 \xi (1-\xi^2)^{-1/4} J_2(kr\xi) d\xi \sim (kr)^2 \times {}_1F_2(2, 11/4, 3, -(k^2r^2/4)), \tag{18}$$

and the first term in (12) is proportional to the square of a different integral ($n = 1$):

$$\int_0^1 \xi (1-\xi^2)^{1/4} J_1(kr\xi) d\xi \sim (kr) \times {}_1F_2(3/2, 11/4, 2, -(k^2r^2/4)). \tag{19}$$

It is seen from (18) and (19) that with increasing of r ($kr \ll 1$) they increase quadratically and linearly, respectively (taking into account that ${}_1F_2(0) = 1$). For small values of the argument ($kr \ll 1$) the linear function is growing faster than quadratic. The second term in (9) and (12) subside at about the same rate, since they have the same maximum (15). Therefore, the first term in (9) adds a smaller positive value to the second decreasing term than the first term in (12) does to the second decreasing term. Thus, the sum of the two terms in (9) decreases faster with increasing r than the sum of the terms in (12). This trend is not impeded but helped by the decrease of the hypergeometric function in (18) and (19).

Indeed, from the form of the hypergeometric function in (17), the coefficients of the argument x are seen to be proportional to $2/k$ in (18) and to $(2k+1)!!/(2k+2)!!$ in (19). That is, given the same value of the function argument (17), each member of a set of the hypergeometric function in (18) is smaller in absolute value than the corresponding term of the hypergeometric function in (19). That is the hypergeometric function in (18) decreases more rapidly with increasing r , than the hypergeometric

function in (19) does. This means that in (19), the linear term grows faster and the hypergeometric function subsides more slowly than grows the quadratic term and recedes the hypergeometric function in (18). From the above reasoning it follows that the diameter of the focal spot for the azimuthal polarization with a singular phase (9) is smaller than the diameter of the focal spot for the beam with radial polarization (12), other conditions remaining the same.

In addition, we show that for small values of the argument of the Bessel functions ($kr \ll 1$) the intensity function (9) and (12) fall down in different ways.

Taking into account (16), instead of (9) and (12) we can write ($E(\theta) = 1$ and $\theta_0 = \pi/2$):

$$I_{az} = 2\pi^2 \left\{ \left[\frac{(kr)^2}{8} \frac{\Gamma(3/4)\Gamma(2)}{\Gamma(11/4)\Gamma(3)} \times {}_1F_2(2, 11/4, 3, -(kr)^2/4) \right]^2 + \left[\frac{\Gamma(3/4)\Gamma(1)}{2\Gamma(7/4)\Gamma(1)} \times {}_1F_2(1, 7/4, 1, -(kr)^2/4) \right]^2 \right\}, \tag{20}$$

$$I_{rad} = 4\pi^2 \left\{ \left[\frac{(kr)}{4} \frac{\Gamma(5/4)\Gamma(3/2)}{\Gamma(11/4)\Gamma(2)} \times {}_1F_2(3/2, 11/4, 2, -(kr)^2/4) \right]^2 + \left[\frac{\Gamma(3/4)\Gamma(3/2)}{2\Gamma(9/4)\Gamma(1)} \times {}_1F_2(3/2, 9/4, 1, -(kr)^2/4) \right]^2 \right\}, \tag{21}$$

It follows from (17) when $x \ll 1$ that

$${}_1F_2(b, c, d, x) \approx 1 + (b/cd)x. \tag{22}$$

Taking into account (22) when $kr \ll 1$ instead of (20) and (21) we can write with accuracy up to series members $(kr)^4$:

$$I_{az} \approx 0.89\pi^2 (1 - 0.29(kr)^2), \tag{23}$$

$$I_{rad} \approx 0.92\pi^2 (1 - 0.26(kr)^2). \tag{24}$$

Note that similarly to (20) and (21) in [12] it was shown that the rate of intensity decrease in the focus for the azimuthal polarization with singular phase is the same as that for the radial polarization (see eqs. (23) and (31) in [12]). But in [12] the authors did not consider a positive contribution of the first summand in braces in (21). This is the summand that makes a slower decrease of the intensity in the case of radial polarization.

From (23) and (24) we see that for small arguments ($kr \ll 1$) the intensity in the focus varies quadratically: in the case of the azimuthal polarization the intensity decreases faster than for the radial polarization. This means

that the intensity of focus for the beam with the azimuthal polarization drops faster (and thus has a smaller focus diameter) than for a beam with radial polarization. This was confirmed by the numerical results reported in [1,3,4].

In the next section light focusing near a microlens surface is considered. Evanescent waves are accounted for in the focus spot forming. The evanescent waves were not taken into account in (1). That is why it is expedient to check whether the focal spot diameter is smaller near the microlens surface when the azimuthal polarization with a singular phase is used instead of the radial polarization.

Numerical comparison of the focusing of light, having passed through different phase plates

Next, we numerically show that, firstly, if we focus the azimuthally polarized beam transmitted through a SPP by a short-zone plate, the diameter of the focal spot is smaller than when we use an aplanatic lens. And secondly, if the azimuthally polarized beam is passed through the phase step with a phase delay of π , the focal spot loses radial symmetry, but is reduced in size.

Let a laser mode with azimuthal polarization fall onto an SPP with transmittance of $F(\varphi) = \exp(im\varphi)$ when $m=1$. The electric vector amplitude has the following projections on the transverse Cartesian coordinates:

$$E_x(r, \varphi) = -r \exp(-r^2/w^2) \sin \varphi,$$

$$E_y(r, \varphi) = r \exp(-r^2/w^2) \cos \varphi. \tag{25}$$

After passing through the SPP the projection of the electric vector (25) will be:

$$E_x(r, \varphi) = -r \exp(-r^2/w^2 + i\varphi) \sin \varphi,$$

$$E_y(r, \varphi) = r \exp(-r^2/w^2 + i\varphi) \cos \varphi. \tag{26}$$

The light field (21) still has the azimuthal polarization and has no longitudinal component of the electric vector. Next, the light field (21) falls on a short-focus binary microlens (zone plate, ZP) (Fig. 1) with a focal length of $f=532$ nm (numerical aperture ZP NA=0.995). The laser light wavelength is $\lambda=633$ nm. The ZP relief depth was equal to 510 nm, and the diameter – 14 μm . The ZP had 12 rings and the central disk and made on a resist with the refractive index 1.52. This ZP was chosen for modeling because it was earlier used for the experiments on the tightly focused laser light [13]. A wavelength of 633 nm (rather than 532 nm) was chosen because at first the micropolarizers were made to convert linear polarization to radial and azimuthal polarizations, and they operate on this wavelength [14]. The focusing of light with amplitude (26) using a ZP (Figure 1) was numerically simulated by FDTD method, realized in FullWave software. The grid discretization step was equal to 0.02 μm . Other simulation parameters: the size of the calculation area is 10x10 μm , the Gaussian beam radius $w=3.5$ μm . Fig. 2a shows the intensity of the beam (25) incident on the SPP. Fig. 2b depicts the phase of the SPP.

Fig. 3 shows the amplitude (a, c) and phase (b, d) for the projections of the electric vector of the light field passed through the SPP and falling on the ZP (see

Fig. 1.): E_x (a, b) and E_y (c, d). It is seen from Fig. 3 that the polarization of the light field after the SPP is no longer azimuthal.

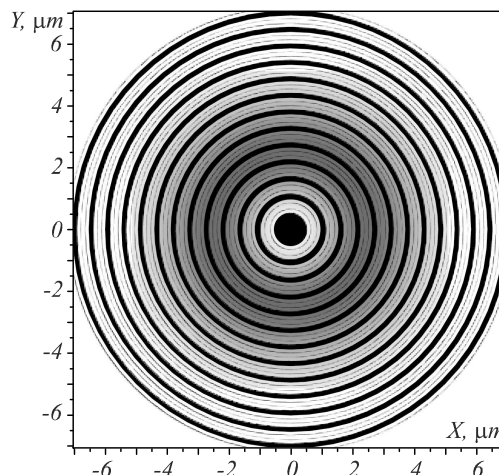


Fig. 1. The view of the simulated ZP in a FullWave window with overlaid intensity of an incident field (negative)

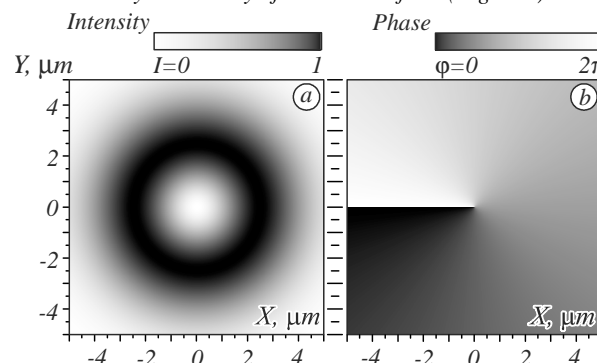


Fig. 2. The intensity $|E|^2$ (negative) of the beam (25) with azimuthal polarization (a) and the phase of the SPP (b)

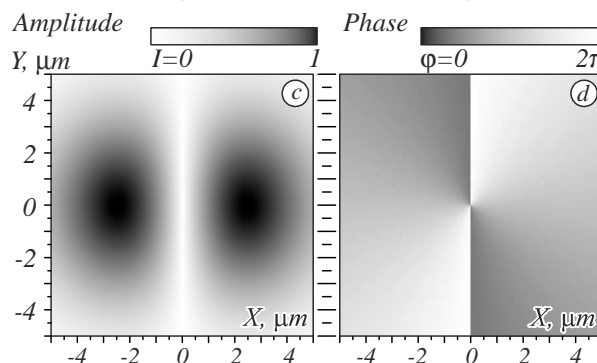
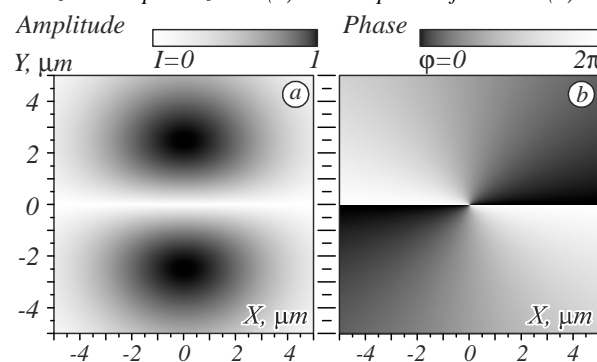


Fig. 3. The amplitude (a) and phase (b) of E_x field and amplitude (c) and phase (g) of E_y field incident on the ZP (Fig. 1)

Fig. 4a shows the intensity profile in the focus of the ZP in Fig. 3 (at a distance $z=40$ nm).

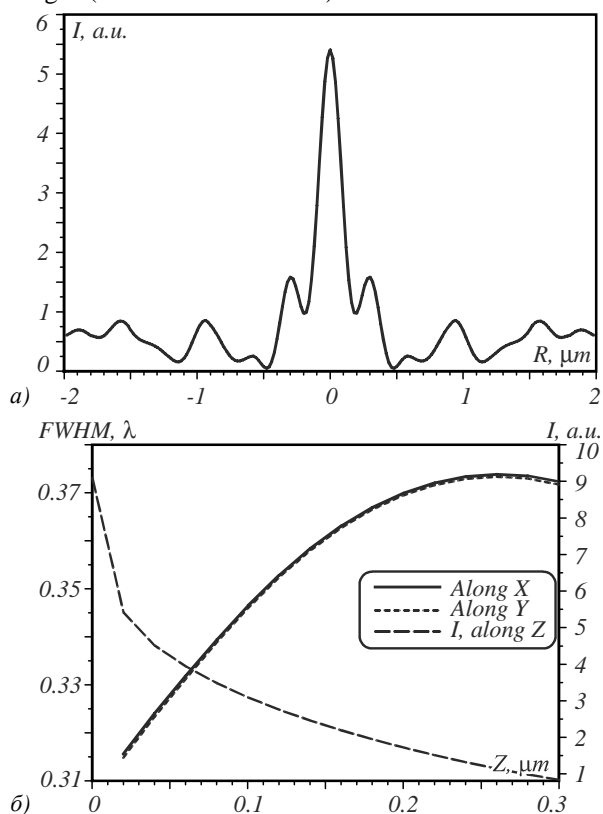


Fig. 4. The radial profile of the intensity in the ZP focus (Fig. 1) of the azimuthally polarized field with a phase singularity (Fig. 3) (a) and the dependence of the focal spot diameter at half intensity (FWHM) on the longitudinal coordinate z (b); dependence of intensity on the optical axis on the Z value

Fig. 4b shows the dependence of the FWHM (in wavelengths) on the longitudinal coordinate z after the ZP. The diameter of the focal spot at a distance $z=40$ nm is equal to $\text{FWHM}=0.324\lambda$, and at the distance $z=200$ nm it is equal to $\text{FWHM}=0.372\lambda$. The maximum intensities at the focus at these distances (in arbitrary units) are: $I_{\text{max}}(z=40 \text{ nm})=5.4$ and $I_{\text{max}}(z=200 \text{ nm})=1.712$. For comparison, the diameter of the focal spot of a Bessel-Gaussian beam with an azimuthal polarization and singular phase focused with an aplanatic lens with a numerical aperture $\text{NA}=1.4$ is $\text{FWHM}=0.34\lambda$ [1, 3]. Up to a calculation error (0.02λ) the diameters of these focal points coincide, but the numerical aperture in [1, 3] is 1.4 times greater.

Note that for the light of wavelength $\lambda=532$ nm incident on the ZP, the size of the focal spot (Fig. 5a) at a distance of $z=500$ nm from ZP is smaller in wavelengths ($\text{FWHM}=0.34\lambda$), than for the wavelength of $\lambda=633$ nm at a distance of $z=200$ nm ($\text{FWHM}=0.372\lambda$). Although in the focus ($z=500$ nm), the focal spot is not round any more (Fig. 5b). The use of the wavelength of 633 nm is due to the perspective of experiments with a micropolarizer [14] designed for this wavelength of light.

Interestingly, the replacement of the SPP by the phase step with phase delay of π leads to a reduction in the focal spot size. In this case, the ZP is illuminated by the light field (25) whose amplitude is multiplied by -1 if the coordi-

nate $y<0$. In this case, the polarization of the light field incident on the ZP is shown in Fig. 6. It can be seen that the polarization is azimuthal, but diametrically opposite points of the field have the mutually opposite direction of the polarization vector. Note that the polarization is not defined on the line of the phase jump (horizontal line).

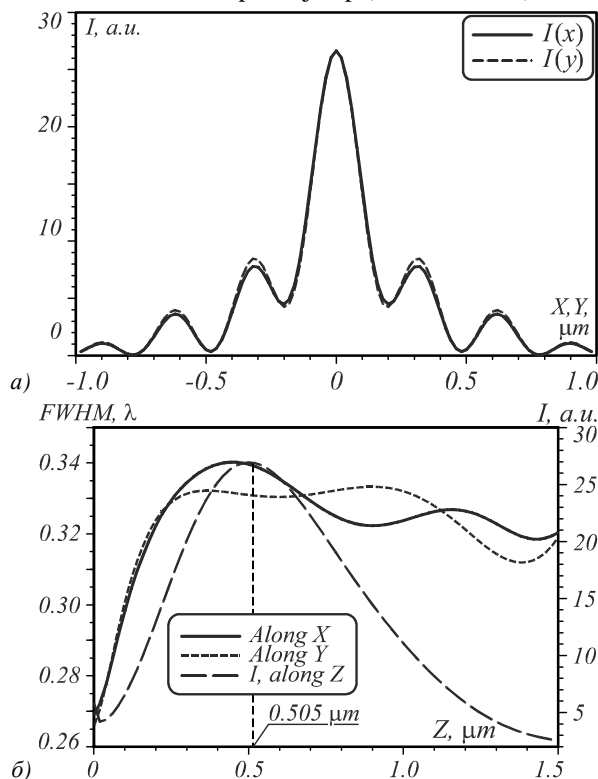


Fig. 5. The radial profile of the intensity in the ZP focus (Fig. 1) of azimuthally polarized field with a phase singularity (Fig. 3) (a) and the dependence of the focal spot diameter at half intensity (FWHM) on the longitudinal coordinate z (b) for the parameters, similar to fig. 4, but the incident light wavelength is 532 nm

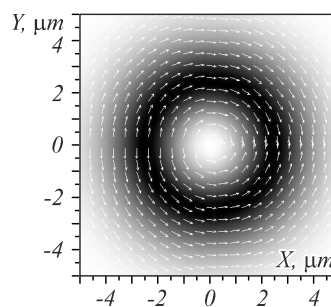


Fig. 6. The intensity $|E|^2$ with arrows that indicate the direction of polarization

Fig. 7 shows the intensity profiles in the focal spot on the x - (solid line) and y -axes (dashed line) at different distances z from the ZP: $z=40$ nm (a) and $z=200$ nm (b).

Fig. 7 shows that the size of the focal spot along a phase jump line (x axis) is smaller than in the direction perpendicular to the phase jump line (y -axis). Although the side lobes along the x -axis adjacent to the focus amount to up to 30% of the maximum intensity.

Fig. 8a shows the dependence of the focal spot size FWHM (in wavelengths) on the x - and y -axes on the dis-

tance to the ZP. The solid curve in Fig. 8a - the focal spot size along the x -axis ($y=0$), the dashed curve - along the y axis ($x=0$).

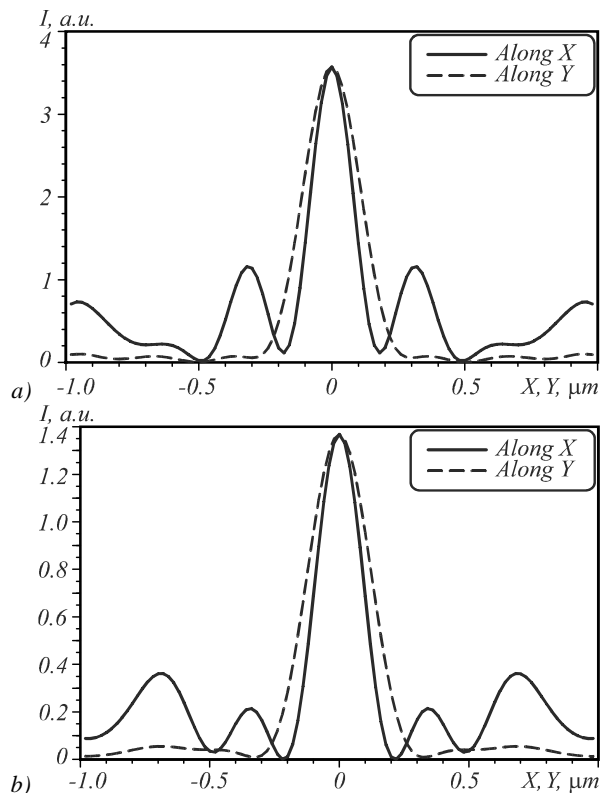


Fig. 7. The central section of the focal spot intensity (solid line along the x axis, dashed line along y axis) at a distance of 40 nm from the ZP (a) and 200 nm (b)

Fig. 8b shows the dependence of the intensity in the center of the focal spot on the distance to the ZP. It is seen from Fig. 8 that at the distance $z=40$ nm, the size of the focal spot at half intensity is equal to $FWHM_x=0.239\lambda$, $FWHM_y=0.273\lambda$, and at the distance $z=200$ nm, the focal spot size is greater: $FWHM_x=0.273\lambda$, $FWHM_y=0.314\lambda$. The maximum intensity in the focus in relative units at these distances is equal to: $I_{max}(z=40\text{ nm})=3.67$ and $I_{max}(z=200\text{ nm})=1.4$.

From the comparison of Fig. 4b and Fig. 8a it can be seen that at distance $z=200$ nm, the focal spot size for a beam with azimuthal polarization that has passed through the phase step, is smaller than $FWHM_y=0.314\lambda$. And the diameter of the focal spot of the beam with azimuthal polarization that has passed through the SPP, is larger than $FWHM=0.324\lambda$.

A comparison with light focusing with radially polarized light can be seen from fig. 9.

All simulation parameters are the same except the incident field, which is describer by

$$E_x(r, \varphi) = r \exp(-r^2/w^2) \cos \varphi,$$

$$E_y(r, \varphi) = r \exp(-r^2/w^2) \sin \varphi. \quad (27)$$

instead of (25).

The size of the focal spot at the same distance ($z=500$ nm) is $FWHM=0.388\lambda$, the focal spot has a round shape. Also the FWHM is wider in λ , it is about 9 nm tighter

in absolute value in comparison with Fig. 5a. It is also seen that the focal spot maximum intensity is 1.8 times higher than for azimuthal polarization with phase singularity.

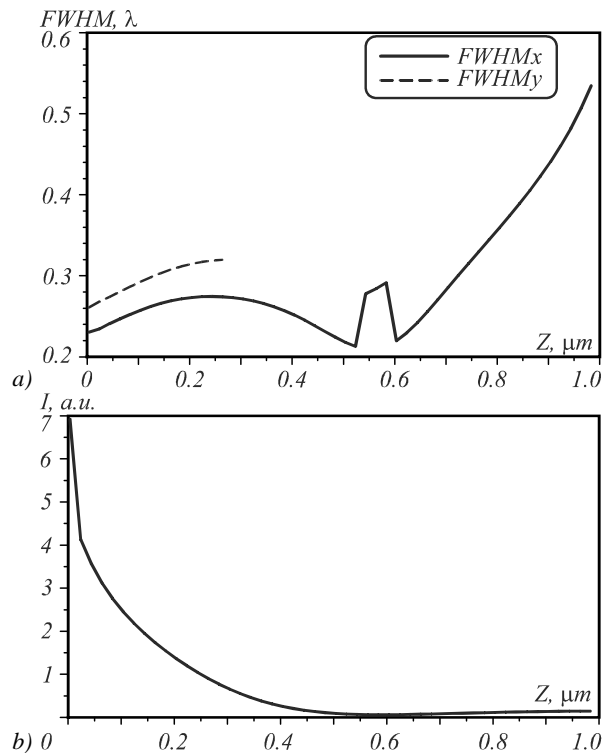


Fig. 8. The size of the focal spot along the axes x (solid line) and y (dashed line), depending on the distance from the ZP (a) and the dependence of the maximum of intensity in the focus on the distance along the z axis (b)

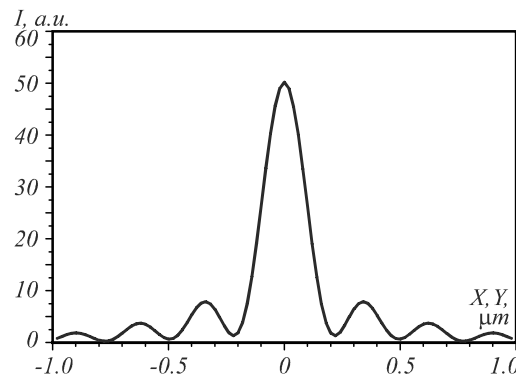


Fig. 9. The radial cross-section of the intensity in the ZP focus, when radial polarization is used. The wavelength is $\lambda=532$ nm, all other parameters are the same Fig. 5

Conclusion

We have obtained the following results. Using Richards-Wolf formulas, the expression for the intensity distribution in the focus of an aplanatic lens for a laser beam with an azimuthal polarization that has passed through a spiral phase plate with the a unit topological charge has been derived. This expression, which consists of the sum of two integral transformations, is theoretically compared with the expression for the intensity in the focus of a beam with radial polarization. It follows from the comparison that the diameter of the focus of the beam with the azimuthal polarization and phase singularity is smaller than the diameter of the focus of

the beam with radial polarization. This is confirmed by the numerical results obtained by other authors. Besides, the light field in the focus of the beam with azimuthal polarization and singular phase has no longitudinal component, and in contrast, the field in the focus of the beam with radial polarization basically consists of a longitudinal component. It is shown numerically using FDTD method, that the diameter of the subwavelength focus ($\text{FWHM}=0.372\lambda$, $\lambda=633$ nm) in the vicinity of a binary zone plate ($\text{NA}=0.995$) for a laser beam with azimuthal polarization and singular phase (passed through a spiral phase plate with the unitary topological charge) is approximately 1.3 times smaller than the focal spot diameter ($\text{FWHM}=0.34\lambda$ at $\text{NA}=1.4$) for the same beam, but obtained using an aplanatic lens with the same numerical aperture.

The width of the focal spot near the surface of the zone plate is equal to $\text{FWHM}=0.34\lambda$ (azimuthal polarization) and $\text{FWHM}=0.39\lambda$ (radial polarization) for the wavelength of 532 nm.

It has been shown numerically that focusing by the zone plate ($\text{NA}=0.995$) of an azimuthally polarized laser beam that has passed through a phase step with a π -phase delay produces an elliptical subwavelength focal spot ($\text{FWHM}_x=0.273\lambda$, $\text{FWHM}_y=0.314\lambda$). The spot size was found to be smaller than that ($\text{FWHM}=0.372\lambda$) formed by the transmission through the spiral phase plate.

References

- [1] Hao X, Kuang C, Wang T, Liu X. Phase encoding for sharper focus of the azimuthally polarized beam. *Opt Lett* 2010; 35(23): 3928-3930. DOI: 10.1364/OL.35.003928.
- [2] Richards B, Wolf E. Electromagnetic diffraction in optical systems. II. Structure of the image field in an aplanatic systems. *Proceedings of the Royal Society A: Mathematical, Physical and Engineering Sciences* 1959; 253(1274): 358-379. DOI: 10.1098/rspa.1959.0200.
- [3] Cheng Z, Zhou Y, Xia M, Li W, Yang K, Zhou Y. Tight focusing of the azimuthally polarized light beam for a sharper spot. *Optics & Laser Technology* 2015; 73: 77-81. DOI: 10.1016/j.optlastec.2015.04.013.
- [4] Li X, Venugopalan P, Ren H, Hong M, Gu M. Super-resolved pure-transverse focal fields with an enhanced energy density through focus of an azimuthally polarized first-order vortex beam. *Opt Lett* 2014; 39(20): 5961-5964. DOI: 10.1364/OL.39.005961.
- [5] Khonina S.N., Karpeev S.V., Generating inhomogeneously polarized higher-order laser beams by use of diffractive optical elements, *J Opt Soc Am A* 2011, 28(10), 2115-2123. DOI: 10.1364/JOSAA.28.002115.
- [6] Wang S, Li X, Zhou J, Gu M. Ultralong pure longitudinal magnetization needle induced by annular vortex binary optics. *Opt Lett* 2014; 39(17): 5022-5025. DOI: 10.1364/OL.39.005022.
- [7] Tian B, Pu J. Tight focusing of a double-ring-shaped, azimuthally polarized beam. *Opt Lett* 2011; 36(11): 1180-1185. DOI: 10.1364/JOSAA.31.001180.
- [8] Xie X, Sun H, Yang L, Wang S, Zhou J. Effect of polarization purity of cylindrical vector beam on tightly focused spot. *J Opt Soc Am A* 2013; 30(10): 1937-1940. DOI: 10.1364/JOSAA.30.001937.
- [9] Khonina SN, Karpeev SV, Alferov SV, Savelyev DA, Laukkanen J, Turunen J. Experimental demonstration of the generation of the longitudinal E-field component on the optical axis with high-numerical-aperture binary axicons illuminated by linearly and circularly polarized beams. *J Opt* 2013; 15(8): 085704. DOI: 10.1088/2040-8978/15/8/085704.
- [10] Prudnikov AP, Brychkov YA, Marichev OI. Integrals and series. Special functions. Moscow: "Nauka" Publisher; 1983.
- [11] Prudnikov AP, Brychkov YA, Marichev OI. Integrals and series. Moscow: "Nauka" Publisher; 1981.
- [12] Khonina SN, Ustinov AV, Pelevina EA. Analysis of wave aberration influence on reducing focal spot size in a high-aperture focusing system. *J Opt* 2011; 13(9): 095702. DOI: 10.1088/2040-8978/13/9/095702.
- [13] Stafeev SS, Kotlyar VV, O'Faolain L. Subwavelength focusing of laser light by microoptics. *J Mod Opt* 2013; 60(13): 1050-1059. DOI: 10.1080/09500340.2013.831136.
- [14] Stafeev SS, Kotlyar MV, O'Faolain L, Nalimov AG, Kotlyar VV. A four-zone transmission azimuthal micropolarizer with phase shift. *Computer Optics* 2016; 40(1): 12-18. DOI: 10.18287/2412-6179-2016-40-1-12-18.

Authors' information

The information about author **Victor Victorovich Kotlyar** you can find on page 634 this issue.

Anton Gennadyevich Nalimov (b. 1980), graduated from Samara State Aerospace University in 2003. He received his Candidate's degree in Physics and Mathematics from Samara State Aerospace University in 2006 on the specialty of Optics. He currently works as an associate professor at the Technical Cybernetics sub-department at Samara National Research University, also holding a part-time researcher's position at the Image Processing Systems Institute of the Russian Academy of Sciences. Candidate in Physics and Mathematics, a coauthor of 95 papers and 3 inventions. E-mail: anton@smr.ru.

Code of State Categories Scientific and Technical Information (in Russian – GRNTI): 29.31.15

Received September 30, 2016. The final version – October 21, 2016.